

Journal of Materials Chemistry B

Accepted Manuscript



This is an *Accepted Manuscript*, which has been through the Royal Society of Chemistry peer review process and has been accepted for publication.

Accepted Manuscripts are published online shortly after acceptance, before technical editing, formatting and proof reading. Using this free service, authors can make their results available to the community, in citable form, before we publish the edited article. We will replace this *Accepted Manuscript* with the edited and formatted *Advance Article* as soon as it is available.

You can find more information about *Accepted Manuscripts* in the [Information for Authors](#).

Please note that technical editing may introduce minor changes to the text and/or graphics, which may alter content. The journal's standard [Terms & Conditions](#) and the [Ethical guidelines](#) still apply. In no event shall the Royal Society of Chemistry be held responsible for any errors or omissions in this *Accepted Manuscript* or any consequences arising from the use of any information it contains.



ARTICLE

Received 00th January
20xx,

Carbon nanostructures enzyme-catalyzed biosensor for bio-electrochemical NADH regeneration

Shuo-Han^a, Jing-bin Zhang^b, Xiong-ying Gao^a, Han-jie Ying^{a*}

Accepted 00th January 20xx

DOI: 10.1039/x0xx00000x

www.rsc.org/

An efficient and biocompatible NADH regeneration system to promote ADH-catalysed oxidation reactions is reported. Carbon nanomaterials allow for an enhanced enzyme attachment within its hierarchical nano-structure. By enzyme protein molecular computer simulation analysis, different electron transfer efficiency on CNTs or GNSs enzyme-catalyzed electrodes result in different electric charge distribution around ADH, which affects its molecular spatial arrangement and three-dimensional conformation. The nanostructure enhances the enzyme-electrode interaction and electron transfer rate. Respectively, 1.4 and 1.9 fold higher current density are reached on CNTs and GNSs *versus* the carbon cloth control for the bio-electrochemical NADH regeneration. Maximum NADH product rates are 2.11 and 3.01 times higher than that on unmodified carbon cloth control. The use of the efficient carbon nanomaterials electrochemical reactor leads to highly conductive three-dimensional cathode for the improvement of bio-electrochemical NADH regeneration, making the nanomaterials an extremely efficient material from an engineering perspective as well.

Introduction

Bio-electrochemical (BEC) sensors have been increasingly utilized in biochemistry, environmental, chemical production and some complex processes over the last few years. The high cost of cofactors (NADH or NADPH) in stoichiometric amounts is one of the bottlenecks, which is creating a rapidly growing demand for new technologies for in situ regeneration of cofactors. Compared with biological, enzymatic, chemical and photochemical methods¹, bio-electrochemical method is of particular interest due to its potentially low cost and no reducing agent addition. Easy product isolation² and no by-products produced might also facilitate BEC to be considered as an interesting option³⁻⁵ to capture and increase the value of the cheap electrical energy produced from renewable sources such as solar, wind and microbial fuel cells. Therefore, BEC is attractive as it can be readily obtainable in large quantities and is more tolerant to economic stress.

Svenja et al. described the different mediators as electron transferring agent by a scalable electrochemical reactor driven NAD(P)⁺ regeneration.⁶ The artificial electron transferring agent is used to reduce overpotential and efficient electron

transfer for conventional electrochemical cofactor regeneration system. However, mediators used in electrochemical systems could lead to enzyme deactivation because of its toxicity to enzymes. Up to date, only a few mediators have been demonstrated the ability to regenerate cofactors, using electricity as the energy source. Even though mediators is an important participator or platform for further electrochemical cofactor regeneration, modification of electrode of known metal oxide electrode capable of BEC, such as SnO₂, has been proposed in order to replace electron transferring agent in the electrochemical cofactor regeneration reaction.³ Similar studies by Irshad et al. demonstrated the ability of some metal electrode (Ti, Ni, Co, Cd) to perform regeneration of NADH over direct electrochemical operation.^{4,5} What's more, many research groups have also studied fundamental aspects of the mechanisms and kinetics of NAD⁺ reduction using a variety of carbon materials.⁷

To the best of our knowledge, electrical contact of NAD⁺-dependent enzymes has been widely used in bioelectronics and biosensor for NADH regeneration.⁸ The immobilization of the proteins in redox polymers associated with electrodes stimulate the bioelectrocatalyzed oxidation of the respective substrates. For sensing proteins, corresponding enzyme molecules generally are low molecular weight, easily immobilized, and with good stability and reproducibility. As a result, applying enzyme molecules as the catalysts in electrochemical biosensors has been widely developed.⁹ Improved enzyme molecules attachment and activity (increasing electron transfer rate) are achieved by modifying the electrode surface by establishing a positively-charged

^a College of Biotechnology and Pharmaceutical Engineering, Nanjing Tech University, Nanjing, 210009, China. E-mail: yinghanjie_njtech@126.com; yinghanjie@njtech.edu.cn

^b Vehicle Institute, Shijiazhuang Railway Transportation School, shijiazhuang, 050057, China.

Electronic Supplementary Information (ESI) available: [details of any supplementary information available should be included here]. See DOI: 10.1039/x0xx00000x

Present address: Nanjing Tech University, No.30 Puzhu Road, Nanjing, 210009, China.

ARTICLE

surface by fixing redox molecules.¹⁰ Bio-electrochemical sensors that utilize enzyme-based electrodes for cofactor regeneration have attracted considerable scientific attention.^{11,12}

However, the BEC reaction mechanisms of enzyme molecules is rather complex. For future industrial purposes, there is still a need to explore the mechanism of enzyme conformation that would be affected by bio-electrochemical reaction system. With the rapid development of computing equipment and technology, protein molecular simulation has achieved great success in many fields.^{13,14} It can provide useful and valuable prediction information that can't be obtained under laboratory conditions. The simulated information would expound mechanism and offer valuable analysis for related research in experiment. Computational study on molecular dynamics simulation of coarse-grained model of isopropylmalate dehydrogenase (IPMDH) protein has been performed successfully.¹⁵ Enzyme protein molecular modeling techniques play an important role in the study of the interaction between the enzyme protein activity and enzyme protein conformation, which will provide theoretical basis for bio-electrochemical analysis.

Optimizing and scaling BEC cofactor regeneration system to practical applications relies on performance improvements while maintaining low costs. Enhancement of kinetics of redox reaction, electron transfer rate at the electrode surface (cofactor-electrode interaction), and cofactor recovery rate will require optimization of several key elements, particularly improved electrode materials, selective oxidoreductase and efficient reactor designs. Moreover, the electrode material must have good stability, excellent conductivity and cost effective. In these applications, carbon nanomaterials, such as carbon nanotubes (CNTs) and graphene nanosheets (GNSs), are commonly fabricated on substrates to serve as working electrode.¹⁶⁻¹⁸ These sensors enhance bio-electrochemical signal responses of the analytes due to their high surface area, strong chemical, heat resistance and minimal reactivity over a wide range of conditions. Carbon nanomaterials are also described as being highly biocompatible allowing for enzyme immobilization and catalysis.¹⁹ Macrostructure enhances the mass transfer to and from the electrode surface while the nanostructure improves enzyme molecules attachment to the electrode and increases the electron transfer rate. These features are extremely important for bio-electrochemical biosensing applications.

To explore the performance of carbon nanomaterials modified electrode for bio-electrochemical sensors of cofactor regeneration, we present a BEC method using enzyme electrode which does not require mediator. We have successfully developed modified-electrodes for electrocatalytic regeneration of enzymatically active NADH. Results show that carbon nanomaterials modified electrode enhanced NADH regeneration within its porous structure. The effect of the macrostructure can effectively enhance current consumption

and NADH bio-electrosynthesis rates. We selected alcohol dehydrogenase (ADH) for use in the biosensing platform. Mechanism of bio-electrochemical cofactor regeneration is analyzed by protein simulation. A series of models are generated to perform molecular dynamics (MD) simulations to investigate the effect of carbon nanomaterials on the structure and activity of ADH

Results and discussion

Fabrication and characterization of enzyme-catalyzed electrode on carbon cloth substrates

The fabrication pathway shown in Fig.1a is to illustrate the enzyme-catalyzed electrode growth. Fabrication of the nanostructures (CNTs or GNSs) layers on the carbon cloth substrates is essential for the later seeding of the electrochemical deposition of the CTS and ADH. Previous investigations indicate that the presence of nanostructure molecules on electrode could influence its electrochemical characterization significantly.²⁰ Nanostructures (CNTs or GNSs) molecules on carbon cloth surfaces can increase the specific surface area and surface energies. We speculate that the CTS might adsorb selectively on nanostructures to promote the enzyme protein growth in these directions.

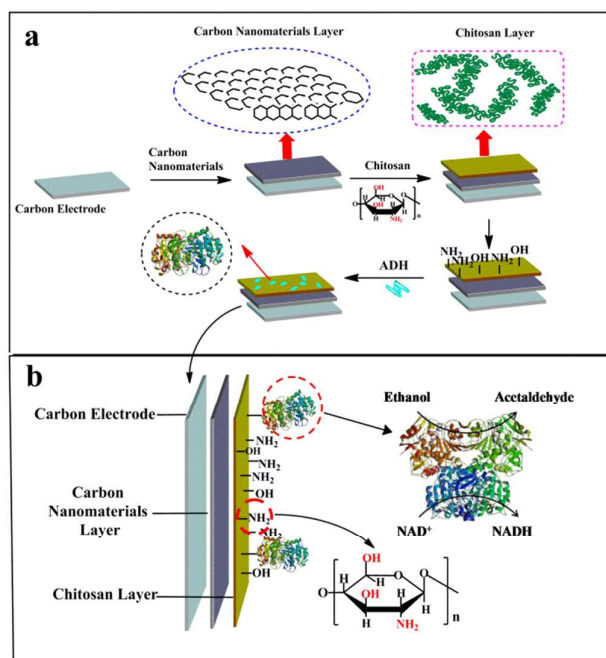


Fig.1 a) Manufacture process of the enzyme-catalyzed electrode. b) Mechanism of bio-electrochemical NADH regeneration with ADH

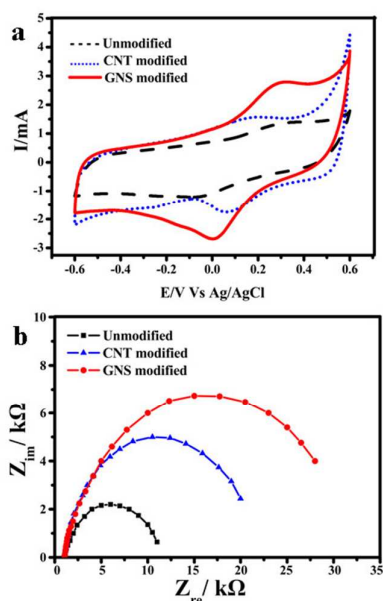


Fig.2 a) Cyclic voltammograms (CV) at the enzyme-catalyzed electrode in 0.2 M PBS (pH 7.5) at scan rate of 20mV/s. b) Nyquist plots from electrochemical impedance spectroscopy (EIS) measurements of various enzyme-catalyzed electrode.

To analyze the electrochemical properties of enzyme-catalyzed electrode, The CV and EIS (Fig.2) were measured to display the oxidation and reduction characterization for three electrodes (each in duplicate): unmodified electrode as control, CNTs modified electrode and GNSs modified electrode. As shown in Fig.2a, three enzyme electrodes can be used for mediator-free NADH oxidation, but the efficiency in the different enzyme-catalyzed electrode is very high. The CV diagrams in Fig.2a display the oxidation and reduction of CNTs-modified enzyme electrode, GNSs-modified enzyme electrode and unmodified enzyme electrode. After the modification of different nanomaterials, a significant increase in the reduction and oxidation peak was observed. Clearly, the GNSs-modified enzyme electrode is the highest one. This is due to the monolayer of flat carbon atoms of the two dimensional structure. This allows more electrons to be exposed on the enzyme electrode surface. The usage of the CNTs or GNSs nanostructured electrode for sensing ADH is measured via electrochemical impedance spectroscopy (EIS), which provides important response signals about the electrode/electrolyte interface, which is employed for sensing ADH by the modified enzyme electrode nanostructures fabricated in this study. In Fig.2b, after subsequent CNTs or GNSs modifications of the enzyme electrode, the semicircles increase due to their efficient electron transfers between the electrolyte interface and the enzyme electrode surfaces. These results indicate that the increased electron transfer efficiency is due to the surface modifications. The GNSs-modified enzyme electrode shows

the best performance in the experiments discussed above. All of the CV and EIS sensitivity results indicate successful achievement of mediator-free bio-electrochemical cofactor regeneration.

Bio-electrochemical regeneration of NADH

After the biosensor started, current consumption is recorded during 120 min for three different electrodes respectively: unmodified electrode as control, CNTs modified electrode and GNSs modified electrode. The cathode potential is fixed at -800 mV. During this period, results of NADH production for the three different types of electrodes are compared to assess efficiency. All datas in Fig.3 have been normalized to the total surface area of the electrodes. This means we consider the total surface area available for enzyme immobilization.

The chronoamperometry is conducted at constant potential of -800 mV to present the cumulative electron consumption (Fig.3a). The electron consumption rate is defined as the slope of $i-t$ curves at different time intervals.⁵ Current density and maximum electron consumption rate recorded on each electrode are summarized in Table 1. On unmodified electrode, there is a slower rate of electrons consumption within the first 40 min. Then, the electron consumption rate increases to $0.152 \mu\text{mol cm}^{-2} \text{min}^{-1}$ over the last 80 min. Similar process is observed on CNTs modified electrode and GNSs modified electrode. On CNTs modified electrode, during the first period of 20 min, the electron consumption rate increases slowly. After the delay, the electron consumption increases to the maximum rate of $0.217 \mu\text{mol cm}^{-2} \text{min}^{-1}$ from 20 min to the end of the test, corresponding maximum cathodic current density of $0.253 \mu\text{A cm}^{-2}$.

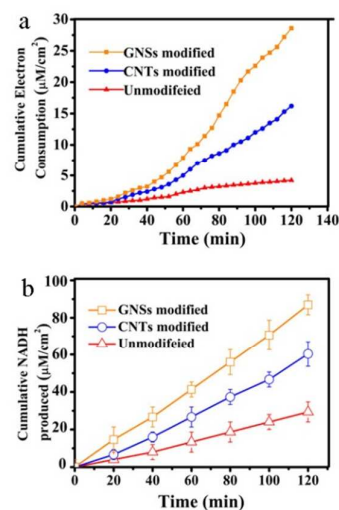


Fig.3 a) Electron consumption over time on enzyme-catalyzed electrode. b) Concentration of NADH generated on enzyme-catalyzed electrode.

Table 1 Maximum electron consumption rates, corresponding current densities and NADH formation rates with different electrodes

	Electron consumption rate ($\mu\text{mol e}^- \text{cm}^{-2} \text{min}^{-1}$)	Current densities ($\mu\text{A cm}^{-2}$)	NADH Product rate ($\mu\text{mol cm}^{-2} \text{min}^{-1}$)
Unmodified	0.152±0.002	0.182±0.001	0.298±0.005
CNTs modified	0.217±0.002	0.253±0.001	0.629±0.004
GNSs modified	0.296±0.001	0.348±0.003	0.897±0.007

Remarkably, the electron consumption rate on GNSs modified electrode is the highest for the test. Results of the maximum current density throughout the 120 min test are in very good agreement to this observation, with maximum consumed rate of $0.296 \mu\text{mol cm}^{-2} \text{min}^{-1}$.

Even though both CNTs and GNSs in the present report and previously described reports are nanomaterials, they are inherently different in nature.¹⁷ Indeed, CNTs modified electrode is not as efficient as the GNSs modified electrode for BEC regeneration of NADH. The GNSs modified electrode performance in BEC leads to higher cathodic current density of $0.348 \mu\text{A cm}^{-2}$. This is about 2 times higher than that on unmodified electrode. Hence, GNSs is an extremely efficient material from this perspective. Obviously, as we can see in this experiment, this value represents the highest current density for cathodic NADH production. The NADH production is obtained throughout the experiments shown in Fig.3b. The maximum product rate is listed in Table 1. The NADH regeneration rates we observed are much greater on the GNSs modified electrode than on the other two electrodes. Consistent with the electron consumption rates shown in Fig.3a, similar increasing of NADH product rates is observed on every electrode. From the start, we found a small amount of NADH production on the unmodified electrode. The maximum NADH product rate can only reach $0.298 \mu\text{mol cm}^{-2} \text{min}^{-1}$. Quite similar trends are then observed on CNTs modified electrode and GNSs modified electrode, with maximum NADH product rate of $0.629 \mu\text{mol cm}^{-2} \text{min}^{-1}$ and $0.897 \mu\text{mol cm}^{-2} \text{min}^{-1}$. During the final period, maximum NADH product rates are 2.11 and 3.01 times higher than that on unmodified electrode. At the last of test, we calculated that, 41.2% and 67.11% of the electrons consumed were recovered in NADH in the CNTs modified electrode and GNSs modified electrode reactors respectively. The difference was mainly caused by the electron transfer efficiency. Morphology structure of flake-like GNSs and line-like CNTs may result in different electrical properties. Some amino acid exposed to ADH protein carrying extra electric charge. They would be attract or reject with the electrode charge. Interaction between these electric charges can affect the ADH protein three-dimensional aspects. From our data in Fig.3 and Table 1, we can concluded that GNSs modified electrode with high electron transfer efficiency had stronger charge force which help ADH protein three-dimensional aspects change. What's more, the changed ADH protein three-dimensional aspects improved the catalytic

activity of ADH for NADH regeneration. More detail of ADH enzyme conformation would be present in protein molecular simulation section.

By gas chromatography, no apparent hydrogen is detected in the reactor, it is believed that the some electrons consumed on enzyme-electrode were used for proton reduction to hydrogen and the produced H_2 may have diffused out of the reactor through the membrane and/or rubber stoppers as reported previously.^{20,21} The results discussed above are a powerful indication of the significant importance of the nanostructure on the electrode to achieve BEC regeneration of NADH. So, we have demonstrated that the performance of mediator-free bio-electrochemical NADH regeneration can be significantly improved using a novel enzyme-catalyzed electrode, CNTs or GNSs. Indeed, from many published reports¹⁶⁻¹⁸ on nanomaterials, when compared to carbon cloth or plates, the total current normalized to the total available surface area would be improved. The main reason for this advantage is the adequate porosity to guarantee efficient mass transport to and from the electrode surface.

The CNTs was previously characterized and showed intertwined fine carbon nanotubes with an average diameter of about 60 nm and pore size within their web of 100nm or smaller.^{19,22} CNTs original macrostructure is not altered in this process, which is critical for development and mass transfer considerations. However, its performance in the BEC for NADH regeneration is inferior compared with GNSs. GNSs holds promise for a wide range of applications due to its outstanding electronic transport properties including high carrier mobility and perfect charge carrier confinement.²³ From the structure, GNSs is only composed with single carbon atoms layer which appears to be of two-dimensional crystals, while CNTs is one-dimensional crystals. In view of the property, the two-dimensional structure (combined the Bottom-up and the Top-down) of GNSs can achieve continuous growth to larger areas, which result in maximisation of the electron transfer rate. That's why CNTs-modified enzyme-catalyzed electrode does not increase the available current density for NADH regeneration as GNSs.

For the novel GNSs, the maximum cathodic current density is $0.253 \mu\text{A cm}^{-2}$ with maximum NADH product rate $0.897 \mu\text{mol cm}^{-2} \text{min}^{-1}$, both of the macrostructure and the nanostructure is believed to be the reason for such a high cathodic current density. Yang et al. who studied regeneration of the nicotinamide cofactor without mediator in very similar experimental conditions to ours, reported about only $0.56 \mu\text{mol cm}^{-2} \text{min}^{-1}$ at -0.95 V with tin oxide electrode.³ Indeed, other mediator-based NADH regeneration systems are not as efficient for bio-electrochemical NADH regeneration. Svenja et al. obtained NADH regeneration with mediator in PBS.⁶ Evidently, even though glassy carbon plate electrode in that report and those described here comprise CNTs or GNSs, they are inherently different in nature. In the current work, CNTs or GNSs is synthesized by directly growing on top of a

highly conductive substrate, which will guarantee both the high conductivity of the electrodes as well as the homogeneous distribution of nanomaterials on the electrode surface. Moreover, the experimental conditions in the previous work are different compared to ours. In this work, we used an enzyme-catalyzed electrode and a higher cathode applied potential of -800 mV. Comparatively, Song et al. obtained a maximum rate of about $0.458 \mu\text{mol cm}^{-2} \text{min}^{-1}$ of NADH^{24} with their platinum nanoparticles materials, versus $0.897 \mu\text{mol cm}^{-2} \text{min}^{-1}$ on GNSs modified enzyme-catalyzed electrode reported in this study. This is an indication of the significant importance of the nanostructure of the electrode material to achieve bio-electrochemical NADH regeneration. To the best of our knowledge, we report here for the first time a higher NADH regeneration rate obtained in an enzyme-catalyzed electrode, an increase compared to previously published data.³⁻⁶

The absence of nanomaterials on unmodified enzyme-catalyzed electrode, plus the observation of lower cathodic current density and NADH regeneration rate in the reactor, strongly suggests that the nanomaterials plays a pivotal role in the high current consumption and bio-electrochemical synthesis performance of the BEC. The much larger electron consumption rate reached on nanomaterials modified enzyme-catalyzed electrode versus unmodified throughout the experiment can be attributed to its large surface available for absorption or the multi-dimensional structure. Additionally, the CNTs or GNSs chemically grown on the carbon cloth surface likely creates a high density of active electron transfer locations, which can then directly interact with the substrate.

All these observations indicate that the nanomaterials are highly biocompatible and support a highly enhanced NADH regeneration rate on the enzyme-catalyzed electrode. Moreover, the high current density obtained suggests that the cofactor-electrode interaction is improved compared to the control, allowing for maximisation of the electron transfer rate. The nanometre scale of the enzyme-catalyzed electrode does increase the available surface area for the interaction between the electrode surface and the electrolyte. This effective nano-scale surface modification with the enzyme-catalyzed electrode is believed to be largely responsible for such enhancement of the current density and NADH regeneration rates achieved in this study with the novel nano-structure electrode material.

Protein molecular simulation to explore the mechanism between enzyme protein conformation and electrocatalysis

The BEC that combines an enzyme-catalyzed reaction with bio-electrochemical cofactor regeneration is performed. Scheme and process of enzyme-catalyzed reaction are shown in Fig.1b. ADH can oxidize ethanol to aldehyde in the presence of NAD^+ , while NAD^+ is reduced to NADH at the same time. In order to explain the relationship between enzyme protein conformation and electrocatalysis, we take advantage of

protein molecular computer simulation method^{28,29} to explore the mechanism of enzyme conformation that would be affected by bio-electrochemical reaction system.

For ADH electrocatalysis system, we set up systematic protein molecular simulation methods for the superimposition of three-dimensional structure displayed in Fig.4. ADH active site is displayed in Fig.5. Three-dimensional structure²⁷ showed that ADH consists of coenzyme binding domain (NAD-binding domain, amino acid residue 143-283) and catalytic core domain (amino acid residue 1-142 and 284-336) (Fig.5). Rossmann folding structure on coenzyme binding domain can combine NAD^+/NADH with its amino acid residue or functional group. It is obvious that the structural changes have taken place in the coenzyme binding domain due to the attendance of adenine ring of NADH. Catalytic core domain rotates by 10° toward the coenzyme binding domain, the later rotates by 1.5° . Adenine is the binding part of coenzyme and enzyme. Hydrogen bond is formed between the adenine-ribose and amino-acid side chains of Asp-223.

Also hydrogen bond can be formed between a hydroxyl of ribose and amino-acid side chains of Thr-48 or His-51.^{28,29} In the ADH electrocatalysis system, hydrogen bond is the proton transfer channel between substrate and enzyme's active site. NAD^+/NADH combining to the ADH by Thr-178, Leu-203 and Met-294 can catalyze the active Zn^{2+} , which formed the ligand with S atom on Cys-46 and Cys-174. Nadolny and Zundel stated that when NAD^+ combined with coenzyme binding domain of ADH, H_2O molecule in the catalytic core domain would be decomposed into OH^- , positive charge can be transferred to His-51 by Zn^{2+} .³⁰

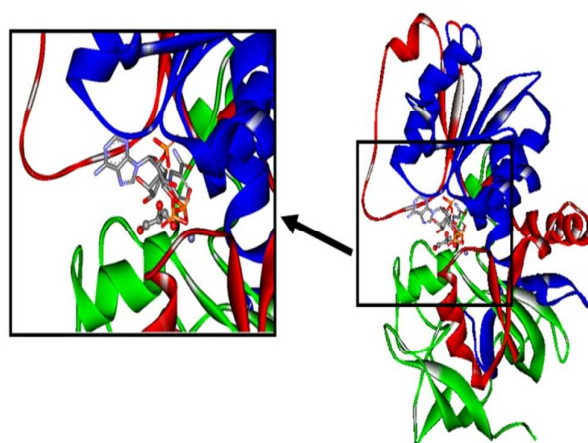


Fig.4 a) Superimposition of three-dimensional structure for ADH combined with cofactor: 143 to 283 (green), 1-142 (blue) and 284-336 (red). The protein is shown in ribbon and cofactor in ball and stick model.

ARTICLE

The equilibrium configurations of ADH adsorbing onto different substrate faces are presented in Fig.1 and Fig.4. NADH regeneration rate on the enzyme-catalyzed electrode with GNSs substrate is higher than that on CNTs substrate. Unmodified enzyme-catalyzed electrode had poorest performance. That's because weak electron transfer efficiency on unmodified enzyme-catalyzed electrode. Covalent bond in carbon atoms of graphitic was different from that in CNTs or GNSs carbon atoms. In cases where the reaction is more efficient on GNSs substrate electrode than on CNTs substrate electrode, it is likely to have a more symmetric and thinner barrier, so that GNSs substrate could make a small, but nonnegligible, contribution to catalysis. An alternative scenario is that the reaction energy does not change but that the barrier is lower on GNSs substrate; in such cases, GNSs substrate will be more compatible with the enzyme-catalyzed processes than on CNTs substrate, making a positive contribution to catalysis.

These results suggest that nanostructure modified electrode can increase the specific surface-area ($S_{\text{BET}} = 243.18 \text{ m}^2/\text{g}$ for GNSs modified, $S_{\text{BET}} = 163.98 \text{ m}^2/\text{g}$ for CNTs modified, $S_{\text{BET}} = 101.69 \text{ m}^2/\text{g}$ for unmodified) and electron transfer rate, resulting in high NADH production rates. CNTs and GNSs (with a two-dimensional lattice of sp^2 -bonded carbon) have markedly different geometrical shapes. CNT has a characteristic line-like structure while GN is flake-like. GNSs are composed of single graphene sheets while a CNT can be viewed as rolled GNSs. GNSs have larger surface area, since the inner surface area of CNTs is lost when GNSs are rolled into CNTs. The larger surface area may provide more possibilities for carrying out chemical reactions. Plane-to-plane contact of GNSs can make electron transfer much more effective on electrode. In addition, the larger surface area of the GNSs can allow stronger interactions than for CNTs electrode and unmodified electrode. GNSs with larger surface area can occupy more free space for movement of enzyme molecule than CNTs. Greater surface area of GNSs can act as more bars in the process of enzyme molecule motion. All this can be defined as stronger physical interactions. In addition, the higher grafting content of GNSs can promote interfacial interactions between enzyme and the substrate.

The differences between CNTs substrate and GNSs substrate are the macrostructure and the nanostructure, which contributed to their different interaction energies and electron transfer efficiency. Different electron transfer efficiency with different electric charge distribution has different effects on protein conformation. Electric charge distribution may contribute to the atomic chemical shift, which affect the molecular spatial arrangement of ADH. Slight changes in ADH conformation correspondingly influence the combination of NAD^+ and coenzyme binding domain. At the same time, catalytic core domain conformation (rotation angle, hydrogen bond or hydrophilia) is also changed slightly, which affect its interaction with ethanol. And the stronger the interaction, the larger the absolute value of the interaction energy.

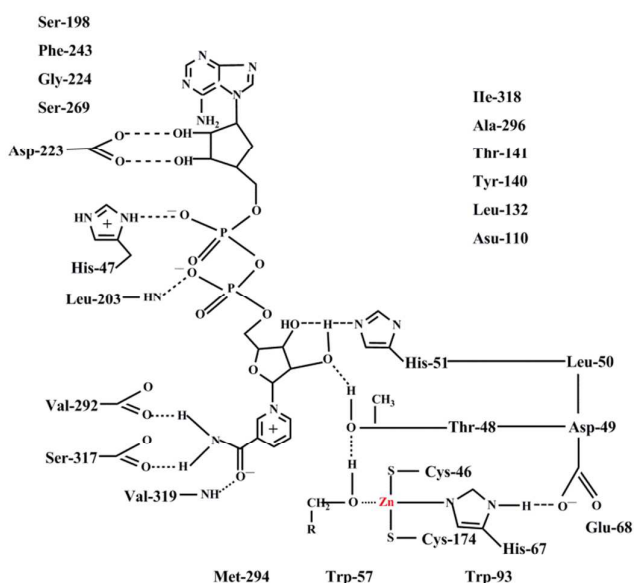


Fig.5 The schematic structure of the active site of ADH.

Conclusions

We have demonstrated in this study that the performance of NADH regeneration can be significantly improved using a novel enzyme-catalyzed nanomaterials electrode. The electron transfer rate between electrode-enzyme (1.9-fold) and the NADH bioproduction rate (3.0-fold) were substantially enhanced on GNSs substrate compared to rough carbon cloth electrode. The results show that the nanomaterials electrode has a very high intrinsic performance as a biocathode material for BEC nanomaterials directly grown on a highly conductive three-dimensional substrate which enables such BEC performance improvements. Therefore the nanostructure increases the electrode's biocompatibility and actually making it possible for enzyme to be fixed, with increased electron transfer. Carbon nanomaterials seem to be a very promising electrode material for practical BEC processes. Future research should focus on elucidating what actually limits the maximally achievable performance by carbon nanomaterials modified substrates.

Experimental

Bio-electrochemical regeneration of NADH

The BEC reactor (Fig.6) consisted of two identical custom designed chambers, each with a volume of 75 mL. The anode and cathode chambers were separated by a proton exchange membrane (Nafion 117) that was sealed with a rubber O-ring. The anode was made of round carbon felt (area = 9 cm^2). The anode chamber used phosphate buffer as anolyte and was

continually gassed with N_2 (0.5 mL/min flow rate) to drive out O_2 . KCl saturated Ag/AgCl reference electrode was inserted into the cathode. Bio-electrochemical regeneration of NADH was performed in a three-electrode configuration for the cathode chamber in order to prevent hydrogen production. During NADH regeneration experiments, the cathode was poised chronoamperometrically at -800 mV. N_2 bubbling was used to maintain anaerobic environment of the cathode chamber. 5 mL gas samples were taken from the cathode headspace using a gas tight syringe. Gas composition was measured on gas chromatography detection

Preparation of enzyme-catalyzed electrode

Composite multilayer electrode presented in Fig.1b was suggested to be the electrocatalytic interface to assemble an electrically contacted, integrated, NAD^+ -dependent enzyme-catalyzed electrode. The enzyme-catalyzed electrode was prepared in one pot by adsorption of alcohol dehydrogenase (ADH, from *Saccharomyces cerevisiae*) and mixture (chitosan and nanomaterials) on the carbon cloth electrode (area = 9 cm^2). In this paper, we respectively selected carbon nanotubes (CNTs) and graphene nanosheets (GNSs) to modify the enzyme-catalyzed electrode. One percent (1%) chitosan (CTS) solution was prepared with Tris-HCl buffer (pH6.0) and then mixed with 2 mg nanomaterials (CNTs or GNSs) with 1 mL of 1% CTS solution together under ultrasonic condition. Then, 16 mg ADH was dissolved in 1 mL of phosphate buffer solution (PBS) solution (pH 7.0). 0.8 mL of viscous nanomaterials (CNTs or GNSs) and CTS suspension was mixed thoroughly with 0.2 mL of ADH solution. Nanomaterials (CNTs or GNSs), CTS and ADH suspension was spread evenly onto the carbon cloth electrode (CCE) surface, the electrodes were allowed to dry for about 24h at 4 °C. Finally the enzyme-catalyzed electrodes were obtained.³¹ Every modified electrode was pierced with a 0.5 mm thick Ti wire that connect with anode.

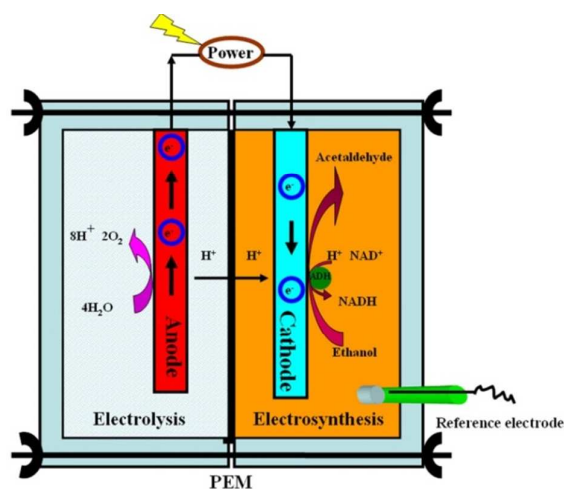


Fig.6 Bio-electrochemical (BEC) reactor schematic diagram

Analysis

Electrochemical characterization of enzyme-catalyzed electrode

Electroanalytical measurements were taken using a conventional three-electrode system for electrochemical analysis. CNTs-modified enzyme-catalyzed electrode, GNSs-modified enzyme-catalyzed electrode and unmodified electrode as control were analyzed. The counter electrode and the reference electrode were a platinum wire and an Ag/AgCl electrode, respectively. Cyclic voltammetry (CV) was performed in PBS (0.2 M, pH 7.5) at room temperature with the enzyme-catalyzed electrode.³ Scan rate was 20mV/s and the range of the potential tested was between -600 and 600 mV. The chronocoulometric response was obtained by chronoamperometry *i-t* curve which was obtained from electrochemical work station. Electrochemical impedance spectroscopy (EIS) experiments (0.1 to 105Hz, 5 mV) were carried out in the PBS solution.¹⁰

Concentration of NAD^+ / $NADH$ determination

NADH regeneration experiments in enzyme-catalyzed electrode were performed with 10 mM ethanol and 1 mM NAD^+ in 0.1 M PBS (pH5.8) with continuous stirring.⁴ The concentrations of NADH were determined by using a NAD/NADH Assay Kit (Germany). All experiments were conducted in triplicate. Data were presented as means and analyzed statistically with SPSS18.0 software. Samples with $p \leq 0.05$ were considered statistically significant by ANOVA. Specific surface area (SSA) of the air-cathode was determined from an N_2 adsorption-desorption experiment with an ASAP2020 surface area analyzer (BET method). All Protein molecular computer simulation details were carried out with software package Gromacs 4.5.5.^{32,33} The structure of ADH was downloaded from the Protein Data Bank. Only one of monomer unit was used in calculations. With the heavy atom positions fixed at their crystallographic positions, hydrogen atoms positions were geometry optimized. Then, the rest of the structure was also kept flexible during the optimization. Hydrogens were added to all atoms, taking care that the nicotinamide mononucleotide moiety unit of the cofactor was reduced at carbon-4. The lowest energy substrate/receptor site conformations for each ligand obtained from docking were submitted to molecular dynamics (conditions, 300 K, 100 ps equilibration, 1 fs step size). Both geometry calculations and conformations for each compound from docking simulations were performed with the Amber94 force field. In order to explore the conformational space of the ligands, all torsional bonds in substrates were set free to perform flexible docking while the enzyme was kept rigid. Polar hydrogens and Gasteiger charges were assigned by the respective modules.

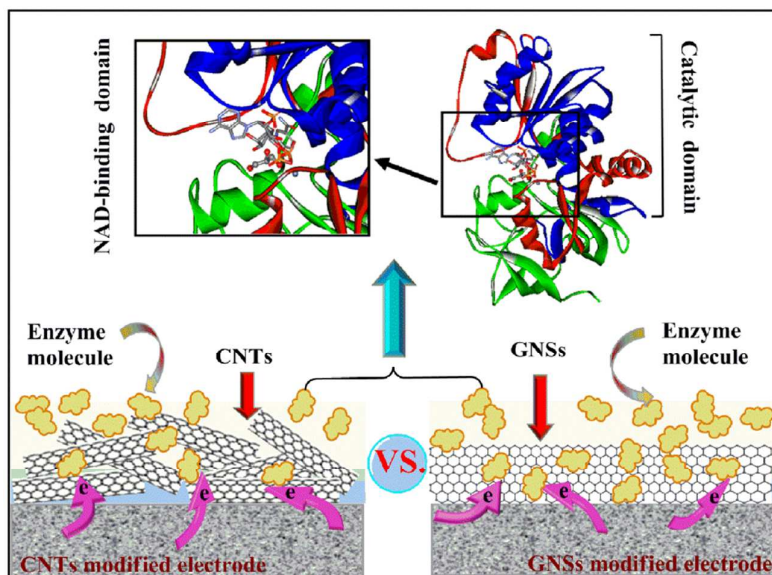
Acknowledgements

This work was supported financially by National 863 Project of China (No. 2012AA021203), the State Key Laboratory of Materials-Oriented Chemical Engineering (ZK201204).

References

- 1 R. Wichmann, D. Vasic-Racki, *Adv. Biochem. Eng/Biotechnol.*, 2005, **92**, 225-260.
- 2 J. Rocha-Martin, D. Vega, J.M. Bolivar, et al., *BMC. Biotechnol.*, 2011, **11**, 101-111.
- 3 Y.H. Kim and Y.J. Yoo, *Enzyme. Microb. Tech.*, 2009, **44**, 129-134.
- 4 I. Ali, A. Gill and S. Omanovic, *Chem. Eng. J.*, 2012, **188**, 173-180.
- 5 I. Ali, T. Khan and S. Omanovic, *J. Mol. Catal. A-Chem.*, 2014, **387**, 86-91.
- 6 S. Kochius, J.B. Park, C. Ley, et al., *J. Mol. Catal. B-Enzym.*, 2014, **103**, 94-99.
- 7 J. Moiroux and P.J. Elving, *J. Electroanal. Chem.*, 1979, **102**, 93-108.
- 8 T.T.N. Boisse, J. Saulnier, N.J. Renault and F. Lagarde, *Anal. Bioanal. Chem.*, 2014, **406**, 1039-1048.
- 9 L. Gorton and E. Domínguez, Wiley-VCH Verlag GmbH & Co KGaA, 2007.
- 10 Y.L. Chen, C.Y. Lee and H.T. Chiu, *J. Mater. Chem. B.*, 2013, **1**, 186-193.
- 11 K.D. Servat, A. Bergel and R. Basseguy, *Bioproc. Biosyst. Eng.*, 2004, **26**, 205-215.
- 12 K. Cheikhou and T. Tzedakis, *AIChE. J.*, 2008, **54**, 1365-1376
- 13 J.J. Gray, *Curr. Opin. Struc. Biol.*, 2004, **14** (1), 110-115.
- 14 K. Ronik, R. Piotr, W. Alan, et al., *Virology*, 2015, **475**, 46-55.
- 15 H. Yosuke, K. Yu, F. Masaki, et al., *JPS. Conf. Proc.*, 016010 2014.
- 16 D.P. Wei, J.I. Mitchell, et al., *Carbon*, 2013, **53**, 374-379.
- 17 L.J. Konwar, J. Boro, and D. Deka. *Renew. Sust. Energ. Rev.*, 2014, **29**, 546-564.
- 18 L.P. Zhang, C. Eva, S. Philippe, et al., *Catal. Today.*, 2014, **235**, 33-40.
- 19 V. Flexer, J. Chen, B.C. Donose, et al., *Energ. Environ. Sci.*, 2013, **6**, 1291-1298.
- 20 L. Jourdin, S. Freguia and B.C. Donose, *J. Mater. Chem. A.*, 2014, **2**, 13093-13102.
- 21 A.W. Jeremiasse, H.V.M. Hamelers, et al., *Bioelectrochemistry*, 2010, **78**, 39-43.
- 22 J. Chen, A.I. Minett, Y. Liu, et al., *Adv. Mater.*, 2008, **20**, 566-570.
- 23 A.K. Geim and K.S. Novoselov, *Nat. Mater.*, 2007, **6**, 183-191.
- 24 H.K. Song, S.H. Lee, K. Won, et al., *Angew. Chem.*, 2008, **120**, 1773-1776.
- 25 B.P. Ling, S.W. Bi, et al., *J. Mol. Graph. Model.*, 2014, **50**, 61-70.
- 26 Y.S. Shi, Z.X. Ming, et al., *J. Mol. Graph. Model.*, 2014, **50**, 71-77.
- 27 K. Mlejnek, B. Seiffert and T. Demberg, *Appl. Microbiol. Biotechnol.*, 2004, **64**, 473-480
- 28 P.E. Smith and J.J. Tanner, *J. Am. Chem. Soc.*, 1999, **121**, 8637-8644.
- 29 C. Anthony and P. Williams, *Biochim. Biophys. Acta.*, 2003, 1647, 18-23.
- 30 C. Nadolny and G. Zundel, *Eur. J. Biochem.*, 1997, **247**, 914-919.
- 31 J. Roche, K.G. Serrano, O. Reynes, et al., *Chem. Eng. J.*, 2014, 239, 216-225.
- 32 D.V.D. Spoel, E. Lindahl, B. Hess, et al., *Gromacs User Manual version 4.0*, www.gromacs.org, 2005.
- 33 D.V.D. Spoel, E. Lindahl, B. Hess, et al., *J. Comput. Chem.*, 2005, 26, 1701-1718.

A table of contents entry



Carbon nanostructures enzyme-catalyzed biosensor with enzyme molecular computer simulation for bio-electrochemical NADH regeneration